Journal of Applied Sciences

ISSN 1812-5654

Journal of Applied Sciences 15 (2): 184-194, 2015
ISSN 1812-5654

ansinet
Asian Network for Scientific Information

RESEARCH ARTICLE OPEN ACCESS

DOI: 10.3923/jas.2015.184.194

Weak Imposition of Essential Boundary Conditions in Isogeometric Analysis of Depth Averaged Advection Dispersion Equation

[1]Ali Hekmat, [2]Airil Yasreen Bin Mohd Yassin, [3]Zulkifli Bin Yusop and [1]Mohammdhossein Kashefizadeh
[1]Department of Hydraulics and Hydrology, Faculty of Civil Engineering, Universiti Teknologi Malaysia, Malaysia
[2]Department of Structure and Material, Faculty of Civil Engineering, Universiti Teknologi Malaysia, Malaysia
[3]Water Research Alliance (IPASA), Faculty of Civil Engineering, Universiti Teknologi Malaysia, Malaysia

ARTICLE INFO
Article History:
Received: October 07, 2014
Accepted: November 20, 2014

Corresponding Author:
Ali Hekmat,
Water Research Alliance (IPASA) C07,
Universiti Teknologi Malaysia (UTM),
Skudai, Malaysia
Tel: +60176259750

ABSTRACT
The “depth averaged advection dispersion” equation is the governing equation in two-dimensional (2D) modelling of contaminant transport in shallow open channel flows. Isogeometric analysis (IGA) is a good method used for accurate geometrical modeling and approximation of the solution space. So, the aim of this study is to conduct the IGA of the depth averaged advection dispersion equation. Due to the non-interpolatory nature of NURBS basis functions the properties of Kronecker Delta are not satisfied, thus imposition of the essential BCs needs special treatment. Therefore, in order to improve the accuracy of the IGA in solution of depth averaged advection dispersion equation, the essential BCs are imposed in three weak forms, including: The Least Square Method (LSM), Lagrange Multiplier Method (LM) and the Penalty Method (PM). For this purpose, the numerical modeling is initially developed and the lateral diffusion problem is solved for a rectangular straight channel and the results of three models are compared with each other. Results indicate that the LSM has the best accuracy while the PM has the poorest. Likewise, despite accurate results, the system of the equation suffers from dimensional enlargement in LM which requires more calculation time. Moreover, in the case of skew advection, adapting the LM produces lower RMSE value and thus more accurate results in contrast to the strong enforced essential BCs in classical FEA and IGA solutions.

Key words: Isogeometric analysis, advection diffusion equation, river mixing lagrange multiplier method, least square method, penalty method

INTRODUCTION

Since analytical solutions generate poor results in terms of accuracy in modeling of the contaminant transport in open channel flows, several researches have employed numerical modeling methods as the alternative solution. The “depth averaged advection dispersion” equation is the governing equation in two-dimensional (2D) modelling of contaminant transport in shallow open channel flows (Fischer *et al*., 1979; Rutherford, 1994). Numerical methods such as Finite Element Method (FEM) are usually incorporated with other models to approximate the solution of the contaminant transport problem in large rivers (Lee and Seo, 2010).

A previous study developed a 2D model with a modified governing equation using FEM and solved the depth averaged advection dispersion equation. Lee and Seo (2007) incorporated a numerical model with FEM to treat the complex geometry of the rivers. Their model was based on the Streamlined Upwind Petrov-Galerkin (SUPG) formulation. They developed a 2D depth advection dispersion model in the Han River, Korea. Seo *et al*. (2008) proposed an FEM model based on a 2D depth averaged mass transport equation and utilized a vertical velocity profile and depth averaged velocity field in order to estimate dispersion coefficient tensors. In all of the above studies, the basis functions were typically interpolatory and have drawbacks associated with them. Interpolatory basis functions suffer from poor representation of exact geometry and accuracy of solution (Cottrell *et al*., 2009). In order to improve the accuracy of the FEM solution as well as the stability of the solution scheme, three solutions can be employed (Cottrell *et al*., 2009). The first solution is improvement of the finite element spaces. The second solution is application of the appropriate variational methods, such as a classical "Stabilized method" (Brooks and Hughes, 1982) The third is to improve both aforementioned solutions (Hughes *et al*., 2005). In respect of the improvement of the finite element spaces, employing the recently proposed methods in which use the NURBS basis functions is incumbent. In this respect, IGA method is based on NURBS basis functions; has some similarities with Finite Element Method (FEM) and incorporates some of the features of Computer Aided Design (CAD) tools. The IGA is a good method to use for accurate geometrical modeling and approximation of the solution space (Cottrell *et al*., 2009). Due to non-symmetric matrix of the advection problem term, the best approximation is not achieved. Therefore, Streamwise Upwind Petrov Galerkin (SUPG) is a useful method to use for stabilized formulation of IGA in fluid analysis (Hughes *et al*., 2005). SUPG is a residual-based modification of the Galerkin method, thus it is capable of increasing the stability without degrading accuracy (Brooks and Hughes, 1982). In the present study the Isogeometric analysis of the depth averaged advection dispersion equation is conducted by SUPG as one of the classical stabilized methods.

In comparison with the conventional FEMs, the IGA method has several advantages such as simple and systematic refinement strategies, exact representation of common engineering shapes, robustness and superior accuracy (Hughes *et al*., 2005). Despite its advantages, the IGA suffers from some weaknesses, the most significant of which arises from the imposition of essential BCs; where due to the non-interpolatory nature of NURBS basis functions, the properties of Kronecker Delta are not satisfied (Piegl and Tiller, 1997; Cottrell *et al*., 2009; Shojaee *et al*., 2012) and this behavior causes a slight smear of the lifting. This phenomenon implies that the imposition of the essential BCs needs special treatment. Bazilevs and Hughes (2007) asserted that problems associated with boundary layer phenomena, adding terms to the variational equation to achieve the weak imposition of BCs will eliminate the spurious oscillations associated with traditional strongly imposed conditions. In recent years, a wide range of techniques have been developed for the implementation of essential BCs in numerical methods. Fernandez-Mendez and Huerta (2004) categorized these techniques in two main categories. The first category includes methods based on modifications of the weak form, such as LM (Belytschko *et al*., 1994), PM (Zhu and Atluri, 1998) and Nitsche's method (Babuska *et al*., 2003; Griebel and Schweitzer, 2003) and LSM which is applied by De Luycker *et al*. (2011) and Mitchell *et al*. (2011) for weak imposition of general inhomogeneous Dirichlet BCs in X-FEM and IGA, respectively. The second category includes methods based on modifications of the interpolation shape functions (Gosz and Liu, 1996; Huerta and Fernandez-Mendez, 2000).

Thereby, in the present study several weak form methods are utilized in order to impose essential BCs. The main contribution of this study is to analyse the depth averaged advection dispersion equation in order to model solute transport in open channel flows. In order to improve the accuracy of the IGA in solution of depth averaged advection dispersion equation, the essential BCs are imposed in the weak form by application of the LM, PM and LSM.

MATEMATHICAL MODELLING OF GOVERNING EQUATION

Governing equation: Fischer *et al*. (1979) developed a 2D theoretical model of shear dispersion in a tensor form which was applied to skewed shear flows with velocity profiles in two directions by using Taylor's method:

$$\frac{\partial c}{\partial t}+u\frac{\partial c}{\partial x}+v\frac{\partial c}{\partial y}=\frac{\partial}{\partial x}\left[D_{xx}\frac{\partial c}{\partial x}+D_{xy}\frac{\partial c}{\partial y}\right]+\frac{\partial}{\partial y}\left[D_{yy}\frac{\partial c}{\partial x}+D_{xy}\frac{\partial c}{\partial y}\right] \quad (1)$$

where, c is the depth-averaged concentration; H is the local depth of flow; T is the temporal variable; q = (u, v) is the depth-averaged fluid velocity vector in the x and y directions, respectively; D the dispersion tensor; Ω a bounded problem domain in the 2D space.

The dispersion tensor D, has the following coefficients expression (Alavian, 1986):

$$\begin{aligned} D_{xx} &= D_L\frac{u^2}{U^2}+D_T\frac{v^2}{V^2},\ D_{xy}=D_{yx} \\ &= (D_L-D_T)\frac{uv}{U^2},\ D_{yy}=D_T\frac{u^2}{U^2}+D_L\frac{v^2}{U^2} \end{aligned} \quad (2)$$

where, D_L, D_T are the longitudinal and transverse dispersion coefficients, respectively and $U=\sqrt{u^2+v^2}$.

In order to implement streamline upwind method, the test function for the advective term is modified with perturbation to the weighting of the second term. If the weak form of depth averaged dispersion equation is multiplied by the series of test functions $(N_1^*, N_2^*, ...N_m^*)$ for m nodes and integrated by parts in the problem domain Ω, leads to:

$$\begin{aligned} &\int_\Omega N_i\left[\frac{\partial(hc)}{\partial t}+\nabla.(hqC)\nabla.(hD,\nabla C)\right]d\Omega+ \\ &\sum_e\int_{\Omega^e}p_i\left[\frac{\partial(hC)}{\partial t}+\nabla.(hqC)-\nabla.(hD.\nabla C)\right]d\Omega \\ &=\int_\Omega\left[N_i\frac{\partial(hC)}{\partial t}+N_i\nabla.(hqC)\right]d\Omega+\int_\Omega(hD.\nabla C).\ \nabla N_i d\Omega \\ &+\sum_e\int_{\Omega^e}p_i\left[\frac{\partial(hC)}{\partial t}+\nabla.(hqC)\right]d\Omega=\int_{\Gamma_2}w_i hgo \end{aligned} \quad (3)$$

N*(x) is the necessary test function of the SUPG formulation. The test function can be divided into continuous and discontinuous terms as given in Eq. 4 (Piasecki and Katopodes, 1999; Seo *et al*., 2008):

$$\begin{aligned} N^* &= N + p \\ p &= \frac{|u|\Delta x + |v|\Delta y}{\sqrt{15U}}\left(u\frac{\partial N}{\partial x} + \frac{\partial N}{\partial y}\right) \end{aligned} \tag{4}$$

where, N is a continuous NURBS basis function and p is the contribution of discontinuous streamline upwind.

Overview of the IGA: NURBS basis functions are weighted functions that originate from B-spline interpolation. The B-spline functions are defined as a series of non-descending real numbers called a knot vector. Knot vector is presented by:

$$\xi = \{\xi_1, \xi_2, ..., \xi_{n+p+1}) \tag{5}$$

where, ξ is the i-th knot value, n and p are the number and the order of basis function defined on the knot vector, respectively. The half open interval $[\xi_i, \xi_{i+1}]$ is called knot interval. If $\xi_i = \xi_{i+1}$, then the length of the knot interval is equal to zero. If ξ_1 and ξ_{n+p+1} are repeated p+1 times in knot vector, the resulting knot vector is called open knot vector. The first order B-spline is defined on the vector by:

$$N_{i,0}(\xi) = \begin{cases} 1 & \text{if } \xi_i \le \xi \le \xi_{i+1} \\ 0 & \text{otherwise} \end{cases} \tag{6}$$

And higher order basis functions are recursively defined by:

$$N_{i,0}(\xi) = \frac{\xi - \xi_i}{\xi_{i+j} - \xi_i} N_{i,j-1}(\xi) + \frac{\xi_{i+j+1} - \xi}{\xi_{i+j+1} - \xi_{i+1}} N_{i+1,\, j-1}(\xi) \tag{7}$$

$$j = 1, 2...., p$$

$$I = 1, 2, ..., n+p+1-j$$

where, $N_{i,j}$ is i-th basis function with a j order.

The NURBS basis functions are made from B-spline functions by the following equation:

$$R_{i,p}(\xi) = \frac{N_{i,p}\, W_i}{\sum_{i=1}^{n} N_{i,p}\, W_i} \tag{8}$$

where, w_i is the weight corresponding to ith control point.

Consequently, $R_{i,p}(\xi)$ is concurrently applied to form both the geometry and approximation functions.

$$x_I = \sum_i R_i(\xi) B_i,\ \psi = \sum_i R_i(\xi)\, \psi_i \tag{9}$$

xi indicates the geometry of problem in multi-dimensional term.

Weak methods of imposition of essential BCs: In this section, three different methods of applying uniform inhomogeneous Dirichlet BCs on the physical boundary of a problem in which an embedding domain is used are presented, including the LM, the PM and the global LSM.

LM: The LM has been widely used in various approaches to improve the imposition of essential BCs, such as meshfree methods (Fernandez-Mendez and Huerta, 2004; Nguyen *et al*., 2008), traditional FEM (Babuska, 1973; Gunzburger and Hou, 1992), extended (Moes *et al*., 2006; Bechet *et al*., 2009) and IGA (Shojaee *et al*., 2012). It is a popular application because of its straightforward implementation. LM adds additional terms for the weak form of equilibrium and the LMs are approximated by $\lambda = N_\lambda\, \tilde{\lambda}$ with NURBS curves basis functions N_λ and the test function υ:

$$\Pi\ (\upsilon 1\lambda) = \min\Pi(\upsilon) + \int_{\Gamma d} \lambda(\upsilon - c_d) d\Gamma \tag{10}$$

If the Eq. 10 is discretized, the following matrix equation can be written:

$$\begin{pmatrix} K & Q \\ Q^T & 0 \end{pmatrix} \begin{pmatrix} \tilde{c} \\ \tilde{\lambda} \end{pmatrix} = \begin{pmatrix} f \\ f_\lambda \end{pmatrix} \tag{11}$$

where, f is load vector and the additional entries:

$$Q = -\int_{\Gamma u} N^T N_\lambda d\Gamma \text{ and } f_\lambda = -\int_{\Gamma u} N_\lambda^T \overline{c} d\Gamma$$

where, N are NURBS surface basis functions. Lagrange multipliers $\tilde{\lambda}$ on the interpolation points are defined within the BCs. Unlike Direct Method (DM) and Transformation Method (TM), the LM is not based on separation of control points and is capable of modeling incomplete Dirichlet boundaries (Shojaee *et al*., 2012). If the control points are on essential boundaries, the interpolation points are the control points and if the control points are not located on the essential boundaries, then the image of the control points on the boundaries are considered. However, if stability conditions (inf-sup condition) are satisfied, then selection of the interpolation points and the number of the interpolation points can be independent of place and the number of control points (Babuska, 1973; Brezzi, 1974). In this study, the system of equations involves finding the unknown value of concentration and also the value of λ simultaneously. However, after inputting λ, the dimension of the resulting system of equations is increased and as a result, the solution of the system of equation will be time-consuming. Another crucial problem is that the system of Eq. 11 and the weak form with LM induce a saddle point problem that, in turn, induces difficulties in the arbitrary choice of the interpolation space for c and λ. On the other hand, in order to obtain an acceptable solution, the discretization of the multiplier λ must be accurate enough. However, if the number of Lagrange multipliers λ_i is too large, the resulting system of equations turns out to be singular. In fact, to ensure the convergence of the approximation, the interpolation spaces for the Lagrange multiplier λ and for the principal unknown c must verify the Babuska-Brezzi stability condition as an inf-sup condition.

PM: Similar to the LM, imposition of BCs $c = c_d$ on a boundary Γ_d yields additional terms for the weak form of equilibrium in PM. An additional system of equations is needed to account for the Dirichlet BC as the following terms with test function υ can be chosen such that $\upsilon = 0$ on the Γ_d:

$$C=\frac{1}{2}\beta\int_{\Gamma_d}\left(\upsilon-c_d\right)^2 d\Gamma \tag{12}$$

The discretization of the weak form of Eq. 12 leads to the following system of equations:

$$(K+BM_p)\ C = f+\beta f_p \tag{13}$$

where, M and f_p is defined as Eq. 14:

$$M_{ij}^p=\int_{\Gamma_d} N_i N_j\ d\Gamma,\ f_i^p=\int_{\Gamma_d} N_i\ u_d\ d\Gamma \tag{14}$$

The only important consideration in using PM is the choice of an appropriate penalty parameter β. To impose the BC accurately, considering $\beta \geq 10^3$ is an appropriate value (Fernandez-Mendez and Huerta, 2004), thus this value is applied in this study. Two significant advantages are attributed to PM in comparison with LM. Firstly, unlike the LM, the dimension of the system will not increase in the PM and, secondly, if K is symmetric and Γ is large enough, then PM yields a positive symmetric definite linear system. On the other hand, PM has two significant weaknesses (Fernandez-Mendez and Huerta, 2004). First, the parameter β controls the quality of ensuring the essential BC and the second is the problems of ill conditioning associated with the PM. In simpler terms, the penalty terms simultaneously affect the diagonal and off-diagonal entries of the system stiffness matrix and when the off-diagonal entries are multiplied by a very large number, the system stiffness matrix may consequently become ill conditioned. As a consequence of this phenomenon, the systems of equations become ill conditioned and applicability of LM reduces subsequently.

Global Least Square Method (LSM): LSM is a good method for the orthogonal projection and is capable of approximating the given data from a finite dimensional subspace appropriately. The LSM approximates the global least-squares problem using a collection of decoupled local least-squares problems which significantly contribute in decreasing the computational cost. The concept of Global LSM is to minimize the quantity of Eq. 15 by finding the parameters of the boundary control points:

$$J=\frac{1}{2}\sum_C \| C(X_C)-\bar{C}(X_C)\|^2=\frac{1}{2}\sum_C\left\|\sum_A \Phi_A(X_C)q_A-\bar{C}(X_C)\right\|^2 \tag{15}$$

In Eq. 15, X_C denotes a set of collocation points distributed on the essential boundary Γ_u. Each q_A is the parameter of the control points defining Γ_u and Φ_A represents the NURBS basis functions that are non-zero at X_c. In order to clarify the concept, a case with one collocation point and a quadratic basis is assumed. In such a case, there are 3 non-zero Φ_A at X_c.

Therefore, Eq. 16 will be rewritten as below:

$$J=\frac{1}{2}\|\Phi_1(X_C)q_1+\Phi_2(X_C)q_2+\Phi_3(X_C)q_3-\bar{C}(X_C)\|^2 \tag{16}$$

The partial derivatives of J with respect to q_i are given by Eq. 17:

$$\begin{aligned}\frac{\partial J}{\partial q_1}&=[\Phi_1(X_C)q_1+\Phi_2(X_C)q_2+\Phi_3(X_C)q_3-\bar{C}(X_C)]\Phi_1(X_C)\\ \frac{\partial J}{\partial q_2}&=[\Phi_1(X_C)q_1+\Phi_2(X_C)q_2+\Phi_3(X_C)q_3-\bar{C}(X_C)]\Phi_2(X_C)\\ \frac{\partial J}{\partial q_3}&=[\Phi_1(X_C)q_1+\Phi_2(X_C)q_2+\Phi_3(X_C)q_3-\bar{C}(X_C)]\Phi_3(X_C)\end{aligned} \tag{17}$$

When the condition:

$$\frac{\partial J}{\partial q}=0$$

the following linear system will come up:

$$\begin{bmatrix}\Phi_1\Phi_1 & \Phi_2\Phi_1 & \Phi_3\Phi_1\\ \Phi_1\Phi_2 & \Phi_2\Phi_2 & \Phi_3\Phi_2\\ \Phi_1\Phi_3 & \Phi_2\Phi_3 & \Phi_3\Phi_3\end{bmatrix}_{X_C}\begin{bmatrix}q_1^z & q_1^y\\ q_2^z & q_2^y\\ q_3^z & q_3^y\end{bmatrix}= \begin{bmatrix}\bar{C}_Z(X_C)\Phi_1(X_C) & \bar{C}_y(X_C)\Phi_1(X_C)\\ \bar{C}_Z(X_C)\Phi_2(X_C) & \bar{C}_y(X_C)\Phi_2(X_C)\\ \bar{C}_Z(X_C)\Phi_3(X_C) & \bar{C}_y(X_C)\Phi_3(X_C)\end{bmatrix} \tag{18}$$

By collecting all the NURBS basis at points X_c in a column vector $N(X_c)$, Eq. 19 can be rewritten in a compacted form as below (the control points displacements in x and y directions in q_x and q_y):

$$\left(N(x_C)N(x_C)^T\right)q_x=\overline{C}_x(x_C)N(x_C)$$
$$\left(N(x_C)N(x_C)^T\right)q_y=\overline{C}_y(x_C)N(x_C) \quad (19)$$

By repeating the same analysis for other collocation points x_C on the Dirichlet boundary, the linear system Λq-b is obtained. In this linear system, two different values are assigned to b, one for the x component and the other for the y component. The dimension of A is $n_D \times n_D$, where, n_D denotes the number of control points defining the Dirichlet boundary. By calculating the displacements for these boundary control points, the imposition of the Dirichlet BCs will be treated in the same way as in standard FEM when solving Kc = f.

ISOGEOMETRIC ANALYSIS OF DEPTH AVERAGED ADVECTION DISPERSION EQUATION

Line source: Numerical results of implementation of the IGA are presented in this section. In order to verify the results of the model with the analytical solution, a rectangular straight channel measuring 100 m long and 20 m wide was proposed and the lateral diffusion problem with flow velocity u was solved for this channel using Eq. 20 (Lee and Seo, 2007; Fischer *et al*., 1979):

$$C=\frac{C_o}{2}\left[1-\text{erf}\,(\frac{y-1}{\sqrt{4D_{T^{x/u}}}})\right] \quad (20)$$

Values of different parameters of the simulation are inspired by the study conducted by Lee and Seo (2007). Parameters of the simulation are as follows: Continuous injection concentration, Co = 100 kg m^{-3}; injection width l = 10 m; flow velocity u = 1 m sec^{-1} and flow depth h = 1 m. Likewise, the longitudinal and transverse dispersion coefficients were assumed to be 1.0 m^2 sec^{-1} and 0.1 m^2 sec^{-1}, respectively. The root-mean-square error (RMSE) is calculated by:

$$RMSE=\sqrt{\frac{\sum_{i=1}^{m}(Ci-C_i^2)^2}{m}} \quad (21)$$

Figure 1 compares the results obtained from the IGA with the analytical solution. In the case of linear basis function, the IGA is compared to the analytical solution at points X = 20 m and 100 m. Figure 1 indicates a considerable convergence rate between the IGA and the analytical solution. The results demonstrate the effectiveness of this approach in solving river mixing problems. However, the RMSE value was 8.22 at D_y = 2 and D_x = 2 for the quadratic NURBS basis function. Due to the fact that the essential BC was imposed strongly in this section and NURBS are not able to satisfy the Kronecker delta; imposing essential BCs require special treatment. Therefore, in the next section, the essential BCs are imposed in a weak form via application of PM, LM and LSM methods in order to achieve higher accuracy. It must be mentioned that most practical fluids formulations employ lower-order, typically constant and linear, interpolation of flow variables (Hughes *et al*., 2005).

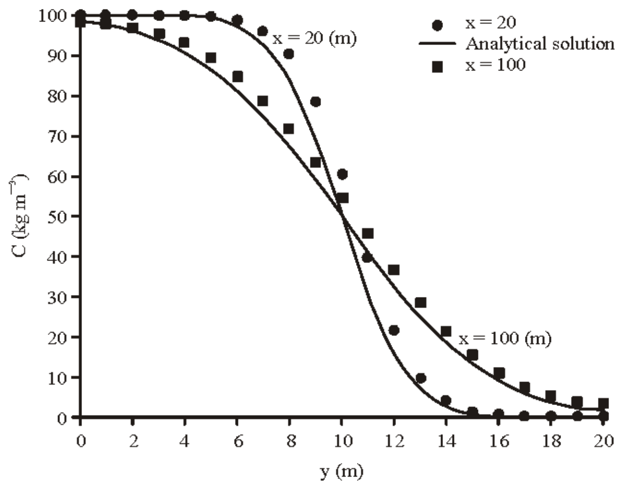

Fig. 1: Numerical results compared with analytical solution at x = 20, 100 m

Likewise, the simple 2D problem in the straight channel with the BC of Eq. 20 can be compared with a one dimensional 1D continuous injection problem (Lee, 2007).

$$C=C_0 \quad \text{on}\,\Gamma_1$$
$$C=0 \quad \text{on}\,\Gamma_3 \quad (22)$$
$$\frac{\partial C}{\partial y}=0 \quad \text{on}\,\Gamma_2 \cup \Gamma_4$$

If the flow is assumed to be plane, then the transverse velocity is zero. Transverse line source problem is considered in this study. So, the transverse concentration gradients are so small that they can be eliminated. In other terms, by assuming the values of V and D_y to be zero, thus the governing Eq. 1 is reduced to Eq. 23:

$$\frac{\partial c}{\partial t}+U\frac{\partial c}{\partial x}-D_x\frac{\partial^2 C}{\partial x^2}=0 \quad (23)$$

Therefore, the 1D solution can be compared to the numerical solution in the 2D domain with the same condition and similar accuracy (Lee, 2007). So the numerical solution of this equation for 2D domains can be compared with the analytical solution of the 1D equation with the BC of Eq. 25:

$$C\,(0,t)=C0,\ C\,(\infty,t)=0 \quad (24)$$

The analytical solution of Eq. 23 with the BC of Eq. 22 comes up with Eq. 25 (Fischer *et al*., 1979):

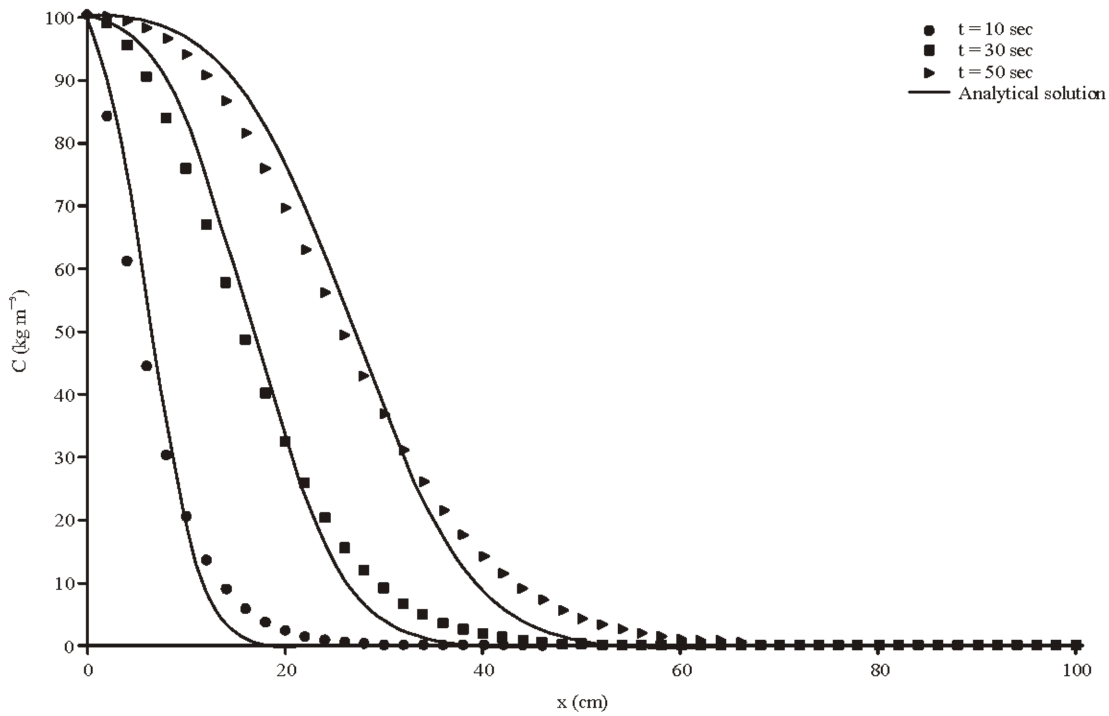

Fig. 2: Comparison of IGA and analytical solution in continuous line source injection at the centre line

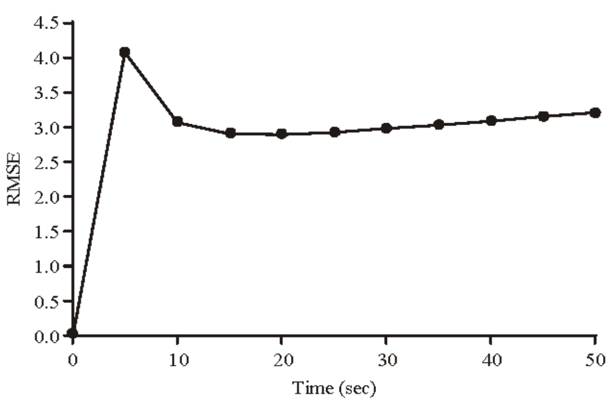

Fig. 3: RMSE error for line source at centre line

$$C=\frac{C_o}{2}\left\{\text{erfc}\left(\frac{x-Ut}{\sqrt{4D_{x^t}}}\right)+\exp\left(\frac{Ux}{Dx}\right)\text{erfc}\left(\frac{x+Ut}{\sqrt{4D_{x^t}}}\right)\right\} \quad (25)$$

Results of employing the model are presented in Fig. 2, 3. Figure 2 shows the results at t =10, 30, 50 sec. As time goes by, the numerical solution by IGA produces a wiggled solution. Although the SUPG method is more accurate when the Peclet number is smaller, there is a wiggle in the results of the IGA. This behavior is similar to the behavior of FEA which is due to the increase in the Peclet number and the predominance of advection. Likewise, Fig. 3 indicates the RMSE trend in the center line of the channel. It is clear in this figure that RMSE has the maximum value of 4.1 in time t = 5 sec. This cause of this significant error in the value of the RMSE is due to the sudden injection of the gradient mass into the flow within the first 5 sec. As time passes, the RMSE remarkably decreases to the value of 3 in time t =10 and after that remains approximately stable.

Instantaneous point source: In order to model the instantaneous pulse injection condition, a M/d=100 kg m^{-1} of mass was released at (x, y) = (0,10) m. The analytical solution of the instantaneous mass injection in the 2D space is given in Eq. 26 (Fischer *et al.*, 1979). Meanwhile, the Heaviside unit step function can be used to define the impulse function:

$$C(x,y,t)=\frac{M/d}{4\pi t\sqrt{D_L D_T}}\exp\left[-\frac{[(x-x_i)-ut]^2}{4D_{L^t}}\right].\exp\left[-\frac{[y-y_i]^2}{4D_{T^t}}\right] \quad (26)$$

Figure 4 shows the comparison of the IGA and analytical results in the pulse injection condition. The results show that in the initial period immediately after realization of the mass, the model develops solutions with significant errors. This behavior is because of the steep gradient of the concentration curve induced from the spatial Dirac delta source treatment. However, this behaviour rapidly changes after the tracer cloud passes through the initial mixing region and the model solution develops results with higher accuracy and smaller errors compared to the exact solution. This implies that, except for the initial mixing region, the model is capable of developing

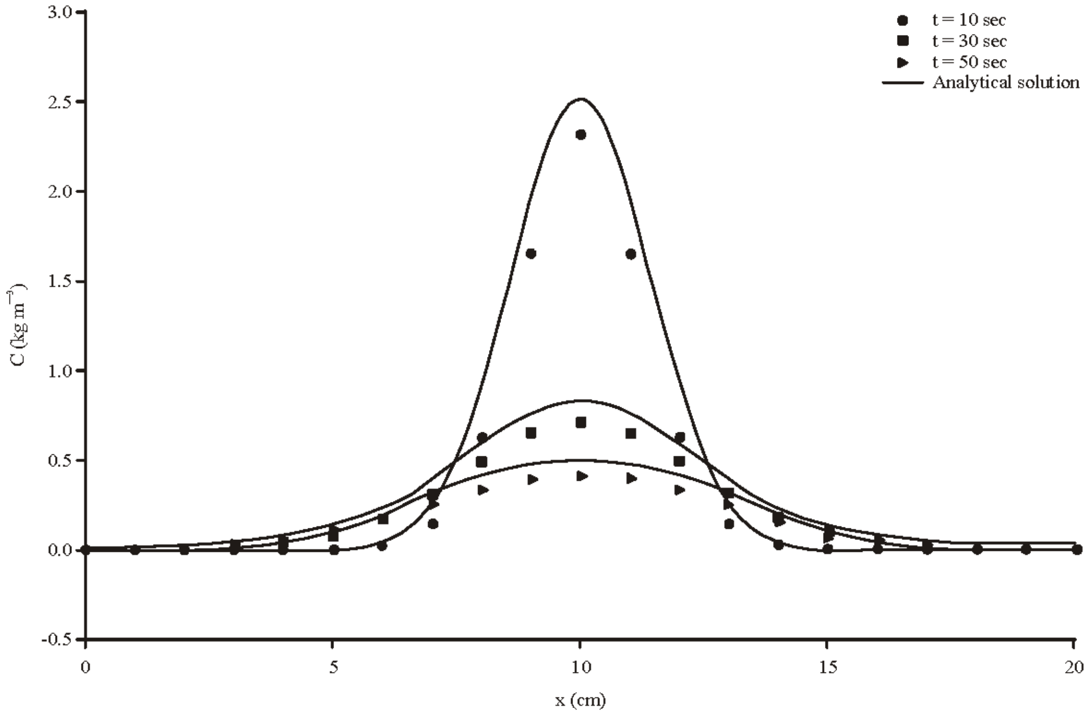

Fig. 4: Comparison of IGA and analytical results in the pulse injection condition

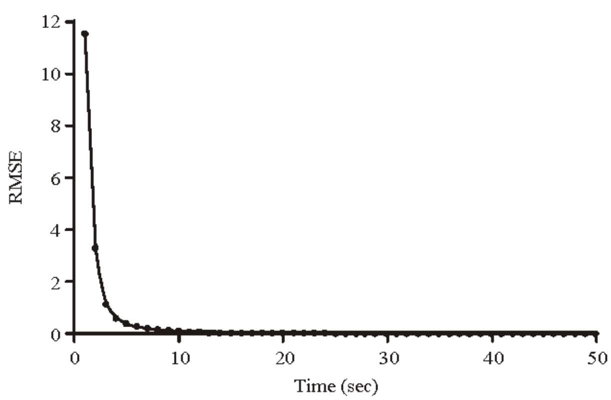

Fig. 5: RMSE for instantaneous point source

a reasonably accurate concentration field for the instantaneously released source. Likewise, Fig. 5 displays that after the initial 5 sec of releasing the pollution the RMSE decreases rapidly. The cause of this significant error is also the steep slope of the initial solution profile. The simulation error, however, decreases rapidly following dispersion of the tracer cloud in the advection. This behaviour implies that, except for the initial period of mass injection, the model is capable of developing a reasonable concentration field for the point released source.

Imposition of inhomogeneous BCs: Results of the study of Lee and Seo (2007) indicated that the RMSE value for line source injection in quadratic at D_y=2 and D_x=2 in FEA is

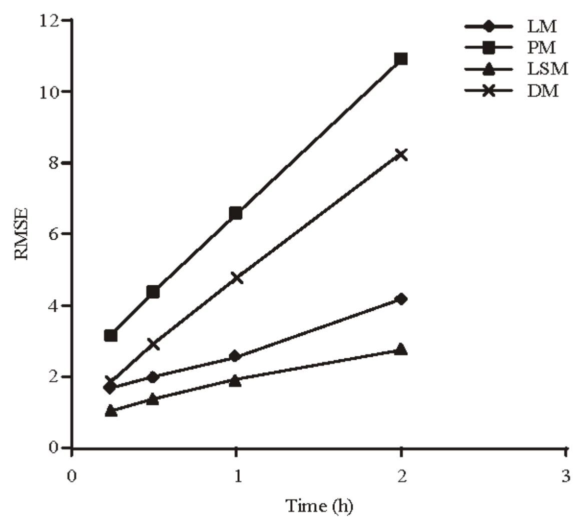

Fig. 6: RMSE error norm for depth averaged

2.754, while, this value is 8.22 in IGA. In this section, the performance of the IGA is improved by weak imposition of the essential BCs via PM, LM and LSM methods. Figure 6 compares the RMSE of PM, LM, DM and LSM versus the size of the mesh (h). As it can be seen in Fig. 6, the LSM has the highest accuracy among all the methods; LM shows a satisfactory accuracy but despite its accuracy, after inputting each λ_i, the dimension of system of equations for LM gets larger. This is the main weakness of LM where this phenomenon causes more time-consumption and can be

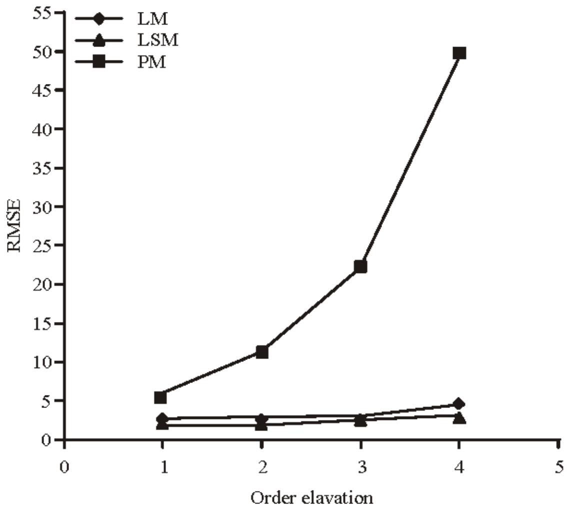

Fig. 7: RMSE error norm for P refinement

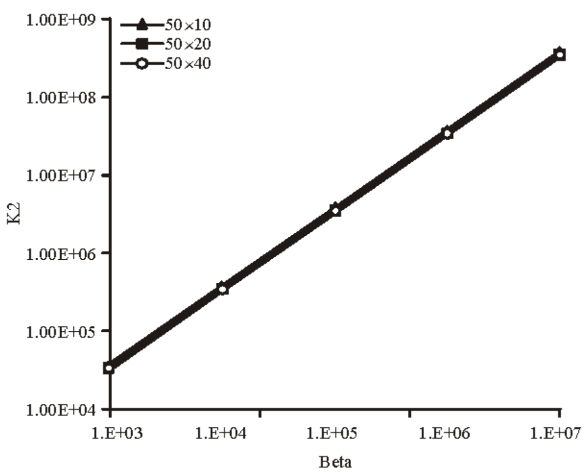

Fig. 8: Evolution of the matrix condition number for the PM

burdensome. PM has the lowest accuracy but, in contrast to LM, the PM does not incur any change in the dimension of the system of equations. Since IGA is able to generate course-mesh inherently, therefore the applicability of the PM is reduced when the coarse discretizations are needed.

Likewise, Fig. 7 shows the variation of RMSE against the elevation order. It can be interpreted from Fig. 7 that the accuracy of the solution using p-refinement strategy trends remarkably downward by increasing the order of the basis functions. This phenomenon implies that p-refinement which always appears with the order elevation, is not a useful strategy in solving the fluid equations. This behavior is in a good agreement with the results of the study of (Hughes *et al*., 2005). The reason for this behavior lies in that the IGA is fundamentally a higher-order approach and a good behavior is unexpected in unresolved interior and boundary layers. In fact, the Gibbs phenomena noted for polynomial-based finite element methods tends to become more pronounced as polynomial order is increased. This is the reason that most practical fluids formulations employ lower-order, typically constant and linear, interpolation of flow variables (Hughes *et al*., 2005).

Table 1: Comparison of the RMSE results for modeling lateral diffusion

RMSE	FEA	LM	LSM
$\Delta y = 1$	2.754	2.022	1.962
$\Delta y = 0.5$	0.756	0.553	0.415

Furthermore, Fig. 7 shows the matrix condition number for increasing values of the penalty parameter for a distribution of 50×20, 50×10 and 50×40 elements. Figure 8 indicates that there is a linear relationship between the increase in the condition number and the penalty parameter. It is evident from Fig. 8 that the ill conditioning of the matrix leads to reduced applicability of the PM. Figure 8 also indicates that even denser discretization cannot reduce the condition numbers. The reason for this phenomenon is obvious in Fig. 8 where all three graphs coincide with each other and by considering the increase in the value of β, the condition number will increase as well.

Table 1 shows the RMSE values for FEA and weak imposition of essential BCs in IGA within quadratic basis function Δy=1 and Δy=0.5. Table 1 implies that by weak imposition of essential BCs using LM and LSM in IGA, the RMSE values are less than FEA; which decreased from 2.754 in FEA to 2.022 and 1.962 in LM and LSM, respectively. It is quite clear that due to not satisfying the Kronecker Delta in IGA, the essential BCs should be imposed in an appropriate weak form method. Thus, the LM can be a good method for imposition of essential BCs in solution of depth averaged advection dispersion equation. However, the system of equation will be time-consuming in LM.

Imposition of homogenous essential BC of skew advection: The longitudinal and transverse directions of the flow direction do not always coincide with the x and y axes of the Cartesian coordinate system. As a result of this phenomenon, velocity and advection borders collide with each other at an angle. Figure 9 depicts the problem of skewed advection with unidirectional uniform flow in a 10×10 m^2 domain. As shown in Fig. 9, the inflow boundary is defined with zero concentration and in the remaining two outflow boundaries, the natural BC of $\nabla C.n_b = 0$ is defined. The mass of M/d = 1000 kg m^{-1} was released at point $(x_i, y_i) = (2, 2)$ m. The analytical solution of the instantaneous mass injection in the 2D space is as follows (Fischer *et al*., 1979; Lee and Seo, 2010):

$$C(x,y,t)=\frac{M/d}{4\pi t\sqrt{D_L D_T}}\exp\left[-\frac{[(x-x_i)\cos\theta+(y-y_i)\sin\theta-ut]^2}{4D_{L^t}}\right]\cdot \exp\left[-\frac{[-(x-x_i)\sin\theta+(y-y_i)\cos\theta]^2}{4D_{T^t}}\right] \quad (27)$$

In real 2D problems, flow direction can skew in any angle. Thus in order to determine the effect of the difference between the element and flow direction in the analytical solution, flow direction is varied for $\theta = 15°$ and $45°$ (Lee and Seo, 2010).

Table 2: Results of the RMSE for imposition of BCs in FEA, IGA and weak imposition of the LM in IGA

	FEA		IGA		IGA (LM)	
Time (sec)	$\theta = 15$	$\theta = 45$	$\theta = 15$	$\theta = 45$	$\theta = 15$	$\theta = 45$
t = 10	5.662	5.243	6.047	5.125	5.095	5.105
t = 20	2.015	2.039	2.192	2.166	1.914	1.835
t = 30	1.086	1.168	1.309	1.403	1.020	1.109
t = 40	0.698	0.779	1.028	1.060	0.677	0.701
t = 50	0.727	0.549	0.928	0.900	0.697	0.521

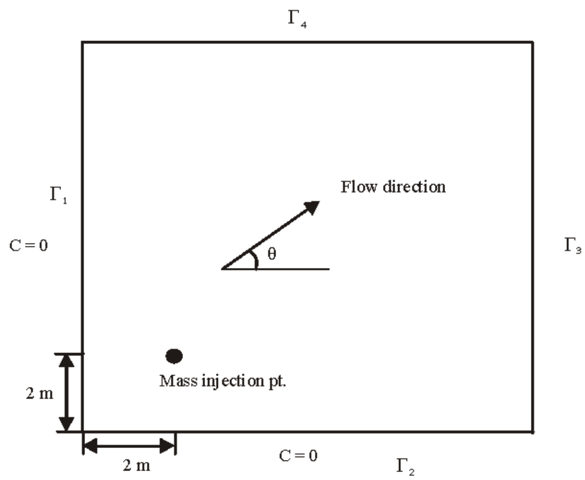

Fig. 9: Schematic of skewed advection with unidirectional uniform flow

For this purpose, in this present study the results of $\theta = 45°$ were compared with the analytical solution at t = 10, 30 and 50 sec after mass injection (Fig. 10). Figure 10a indicates the initial period of mass transport. As can be seen in this figure,unlike the exact solution, the arrival time of the core of the tracer cloud experiences a slight delay which is due to the incapability of the finite difference time integration of the numerical model in following the instant moment of mass releasing completely. As time goes by, the trend of the numerical solution gradually shows convergence to that of the exact solution (Fig. 10b). Despite the numerical solution trend showing a successful convergence to the exact solution after a while, it starts to deviate from the exact solution in the vicinity of the outflow boundary, where the gradient of concentration is zero. However, by replacing the outflow boundary further downstream, this deviation can be reduced (Fig. 10c).

Since in this case, $\bar{c} = 0$ and the linear system of Aq = b will remain unchanged, therefore, in imposition of the LSM, the results will be the same to the initial attempt. Yet, by employing the LM, the results are likely to improve and the RMSE decreases subsequently. Table 2 presents the comparison of the results of FEM, IGA and weak imposition of IGA by LM. It is clear that by imposition of LM the value of RMSE considerably decreases in compare to FEM and IGA. This behavior implies that in employing IGA, imposition of the BCs should be done by an appropriate weak form; and LM is a good method for this purpose. A significant advantage of this behavior is that LM can be useful in the analysis of the rivers with more complicated geometries, where the control points are less likely to coincide the geometry of the channels.

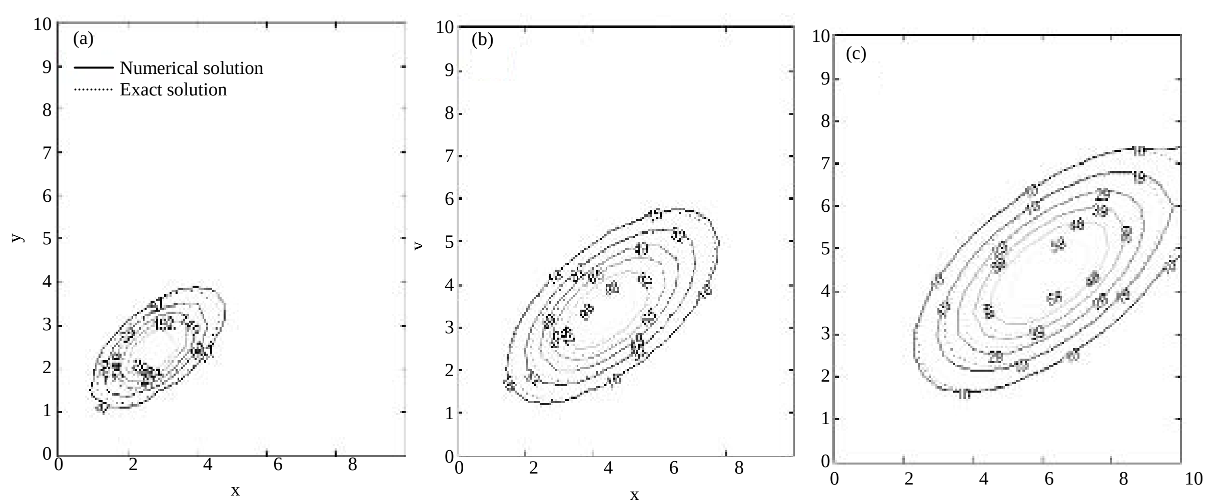

Fig. 10(a-c): Concentration (kg m^{-3}) results for case $D_L = 0.05$ m^2 sec^{-1}, $D_T = 0.01$ m^2 sec^{-1}: (a) t = 10, (b) t = 45 and (c) t = 50 sec

CONCLUSION

In this study, IGA of the depth averaged advection dispersion equation was conducted in an open channel flow based on NURBS basis functions with SUPG employed to stabilize the numerical result. For this purpose, the mathematical formulation of the governing equation was developed and the Dirichlet BC was imposed strongly in a rectangular straight channel, the analytical and numerical results of the implementation of IGA are compared for continuous line source and instantaneous point source. Comparison indicates that despite convergence solution errors, because of not satisfying the Kronecker Delta, the imposition of the essential BC needs special treatment. Therefore, methods LM, PM and LSM were adapted for the weak imposition of essential BCs in depth averaged advection dispersion equation of mass transport of an open channel flow. Results indicate that the LSM has the best accuracy while the PM has the poorest. It was found that despite LM is easy to be adapted and produces accurate results, the system of the equation suffers from dimensional enlargement and it requires more calculation time. Moreover, in the case of skew advection, adapting the LM produces lower RMSE value and thus more accurate results in contrast to the strong enforced essential BCs in classical FEA and IGA solutions. Furthermore, employing the LSM in the homogeneous BC does not incur any change in the results of the skew advection. Results imply that IGA is a good solution in depth averaged dispersion equation, yet since Kronecker Delta is not satisfied, the essential BCs should be imposed by an appropriate weak form and in this respect, LM and LSM are good methods to be employed in order to achieve an accurate solution.

REFERENCES

Alavain, V., 1986. Dispersion tensor in rotating flow. J. Hydr. Eng., 112., 771-777

Babuska, I., 1973. The finite element method with Lagrangian multipliers. Numerische Mathematik, 20: 179-192.

Babuska, I., U. Banerjee and J.E. Osborn, 2003. Meshless and Generalized Finite Element Methods: A Survey of Some Major Results. In: Meshfree Methods for Partial Differential Equations, Griebel, M. and M.A. Schweitzer (Eds.). Springer, Berlinm Germany, ISBN-13: 9783540438915, pp: 1-20.

Bazilevs, Y. and T.J.R. Hughes, 2007. Weak imposition of Dirichlet boundary conditions in fluid mechanics. Comput. Fluids, 36: 12-26.

Bechet, E., N. Moes and B. Wohlmuth, 2009. A stable Lagrange multiplier space for stiff interface conditions within the extended finite element method. Int. J. Num. Meth. Eng., 78: 931-954.

Belytschko, T., Y.Y. Lu and L. Gu, 1994. Element-free Galerkin methods. Int. J. Num. Meth. Eng., 37: 229-256.

Brezzi, F., 1974. On the existence, uniqueness and approximation of saddle-point problems arising from lagrangian multipliers. Math. Mod. Num. Anal., 2: 129-151.

Brooks, A.N. and T.J.R. Hughes, 1982. Streamline upwind/Petrov-Galerkin formulations for convection dominated flows with particular emphasis on the incompressible Navier-Stokes equations. Comput. Meth. Applied Mech. Eng., 32: 199-259.

Cottrell, J.A., T.J.R. Hughes and Y. Bazilevs, 2009. Isogeometric Analysis: Toward Integration of CAD and FEA. 1st Edn., John Wiley & Sons, Ltd., UK., ISBN-13: 978-0470748732, Pages: 360.

De Luycker, E., D.J. Benson, T. Belytschko, Y. Bazilevs and M.C. Hsu, 2011. X-FEM in isogeometric analysis for linear fracture mechanics. Int. J. Num. Meth. Eng., 87: 541-565.

Fernandez-Mendez, S. and A. Huerta, 2004. Imposing essential boundary conditions in mesh-free methods. Comput. Meth. Applied Mech. Eng., 193: 1257-1275.

Fischer, H.B., E.J. List, R.C.Y. Koh, J. Imberger and N.H. Brooks, 1979. Mixing in Inland and Coastal Waters. Academic Press, New York, ISBN: 9780122581502.

Gosz, J. and W.K. Liu, 1996. Admissible approximations for essential boundary conditions in the reproducing kernel particle method. Comput. Mech., 19: 120-135.

Griebel, M. and M.A. Schweitzer, 2003. A Particle-Partition of Unity Method Part V: Boundary Conditions. In: Geometric Analysis and Nonlinear Partial Differential Equations, Hildebrandt, S. and H. Karcher (Eds.). Springer, Berlin, Germany, ISBN-13: 9783540440512, pp: 519-542.

Gunzburger, M.D. and S.L. Hou, 1992. Treating inhomogeneous essential boundary conditions in finite element methods and the calculation of boundary stresses. SIAM J. Num. Anal., 29: 390-424.

Huerta, A. and S. Fernandez-Mendez, 2000. Enrichment and coupling of the finite element and meshless methods. Int. J. Num. Meth. Eng., 48: 1615-1636.

Hughes, T.J.R., J.A. Cottrell and Y. Bazilevs, 2005. Isogeometric analysis: CAD, finite elements, NURBS, exact geometry and mesh refinement. Comput. Meth. Applied Mech. Eng., 194: 4135-4195.

Lee, M.E., 2007. Two-dimensional finite element model for pollutant transport analysis. Ph.D. Thesis, Seoul Natinal University.

Lee, M.E. and I.W. Seo, 2007. Analysis of pollutant transport in the Han River with tidal current using a 2D finite element model. J. Hydro-Environ. Res., 1: 30-42.

Lee, M.E. and I.W. Seo, 2010. 2D finite element pollutant transport model for accidental mass release in rivers. KSCE J. Civil Eng., 14: 77-86.

Mitchell, T.J., S. Govindjee and R.L. Taylor, 2011. A Method for Enforcement of Dirichlet Boundary Conditions in Isogeometric Analysis. In: Recent Developments and Innovative Applications in Computational Mechanics, Mueller-Hoeppe, D., S. Loehnert and S. Reese, Springer, Berlin, Germany, ISBN-13: 9783642174841, pp: 283-293.

Moes, N., E. Bechet and M. Tourbier, 2006. Imposing Dirichlet boundary conditions in the extended finite element method. Int. J. Num. Meth. Eng., 67: 1641-1669.

Nguyen, V.P., T. Rabczuk, S. Bordas and M. Duflot, 2008. Meshless methods: A review and computer implementation aspects. Math. Comput. Simul., 79: 763-813.

Piasecki, M. and N.D. Katopodes, 1999. Identification of stream dispersion coefficients by adjoint sensitivity method. J. Hydraul. Eng., 125: 714-724.

Piegl, L. and W. Tiller, 1997. The NURBS Book. 2nd Edn., Springer-Verlag, Berlin Heidelberg, ISBN: 3540615458, pp: 646.

Rutherford, J.C., 1994. River Mixing. John Wiley and Sons, Chichester.

Seo, I.W., M.E. Lee and K.o. Baek, 2008. 2D modeling of heterogeneous dispersion in meandering channels. J. Hydraul. Eng., 134: 196-196.

Shojaee, S., E. Izadpenah and A. Haeri, 2012. Imposition of essential boundary conditions in isogeometric analysis using the lagrange multiplier method. Iran Univ. Sci. Technol., 2: 247-271.

Zhu, T. and S.N. Atluri, 1998. A modified collocation method and a penalty formulation for enforcing the essential boundary conditions in the element free Galerkin method. Comput. Mech., 21: 211-222.